

Document downloaded from:

<http://hdl.handle.net/10251/47611>

This paper must be cited as:

Lujan Martinez, JM.; Serrano Cruz, JR.; Dolz Ruiz, V.; Sánchez Serrano, J. (2012). Model of the expansion process for R245fa in an Organic Rankine Cycle (ORC). *Applied Thermal Engineering*. 40:248-257. doi:10.1016/j.applthermaleng.2012.02.020.



The final publication is available at

<http://dx.doi.org/10.1016/j.applthermaleng.2012.02.020>

Copyright Elsevier

Keyword Highlights:

1. Evaluate the ideal gas behaviour of R245fa in typical working conditions of an Organic Rankine Cycle (ORC).
2. Compare the ideal behaviour with other simple equations of state for real gas.
3. Decide which equation of state has the highest precision in typical working conditions of an ORC.
4. Derive the most important thermodynamic variables in each equation of state and decide the most accurate equation.
5. Evaluate the specific output energy obtained in a typical ORC using different equation of state compared

# Model of the expansion process for R245fa in an Organic Rankine Cycle (ORC)

J. M. Luján, J. R. Serrano, V. Dolz, J. Sánchez

*Universitat Politècnica de València, CMT-Motores Térmicos, Camino de Vera s/n, 46022 Valencia, Spain.*

---

## Abstract

An Organic Rankine Cycle (ORC) is considered as one of the most environmental-friendly ways to convert different kinds of low temperature energies, i.e. solar, geothermal, biomass and thermal energy of exhaust gases into electrical energy. Two important facts about the ORC must be considered: An organic fluid is selected as the working fluid and a high expansion ratio is usually presented in the machinery due to thermodynamic and efficiency factors. In the past, the pre-design of turbomachinery has been based on the usage of ideal fluid laws, but the real gas effects have a significant influence in the ORC working condition, due to its proximity to the saturation vapor line. In this article, the Equations of State (EoS) (Ideal gas, Redlich-Kwong-Soave and Peng-Robinson) have been evaluated in a typical ORC expansion in order to observe the inaccuracies of the ideal gas model with different thermodynamic variables. Finally an isothermal process followed by an isochoric process is proposed to reproduce the thermodynamic process of the organic fluid expansion by means of simpler equations. In the last point of this paper, several examples of this expansion process have been calculated, in order to analyze the proposed methodologies. It has been concluded that in typical expansion process of ORC (2.5 MPa-0.1 MPa and 1.6MPa-0.1MPa), the PR and RKS equations show deviations between 6% and 8% in specific energy. These deviations are very low compared with the ideal gas equation whose deviations are above 100 %.

*Keywords:* Organic Rankine Cycle, real gas, R245fa, expansion process, equation of state

---

## 1. Introduction

The trends of rising fuel costs and the necessity of reducing CO<sub>2</sub> emissions is forcing governments and industries to focus on the development of low temperature heat energy recovery systems.

Many solutions have been proposed to generate electricity from waste thermal energy produced by industrial processes and power plants. Generally, the conventional methods for energy recovery in industrial process are economically infeasible due to the low temperature of the heat source (less than 500 K). Among the proposed solutions, the Organic Rankine Cycle (ORC) is the most widely used [1]. The ORC consists of the classical steam generation in a Rankine cycle using an organic working fluid instead of water. The organic fluid is usually characterized by low

---

\*V. Dolz. CMT-Motores Térmicos, Universitat Politècnica de València, Camino de Vera s/n, 46022 Valencia, Spain.  
Phone: +34 963877650 Fax: +34 963877659 e-mail: vidolrui@mot.upv.es

saturation temperatures and by a saturated vapor line with positive slope in the  $T - s$  diagram [2],[3]. This positive slope prevents the formation of a two-phase mixture during the expansion process through the turbine.

R245fa, also known as 1,1,1,3,3-Pentafluoropropane, is usually selected as the working fluid in ORC with low temperatures of heat sources due to different factors like its critical temperature, critical pressure and its pressure at 298 K (near atmospheric conditions). The ORC working conditions are usually between 300 K (condensation process) and 450 K (evaporation process) due to the low temperatures of the heat sources. The pressures associated to these temperatures are about 0.1 MPa and 2.5 MPa. These working conditions with high pressures near the saturated vapor line cause a deviation between the real and ideal gas behavior. This deviation is generated by neglecting molecular volume and intermolecular forces of the gas when the ideal gas model is considered. It is well known that when these organic fluids are studied, the ideal gas hypothesis can be regarded only under low temperature and low pressure conditions [4].

In these technologies for the recovering of waste energy, the design and the evaluation of expander machines are two of the most important aspects to achieve high efficiencies in the cycle. Typically, calculations with steam turbines using the ideal gas law are leading to acceptable results. But in this kind of technology, when organic fluids are considered, the differences between the ideal fluid model and the real thermodynamic behavior are quite important. In addition, if high expansion ratio is required, the supersonic impulse turbine (Laval Turbine) is the best choice as results of its easy regulation and cheap maintenance. A supersonic Laval nozzle in the stator is used to accelerate the flow to supersonic condition. This high kinetic energy is converted into torque on the rotor. The consideration of a real gas model is essential in this type of turbines when they are used with organic fluids. Using simple models like the ideal gas one can introduce inaccuracies unacceptable to the study of the organic Rankine cycles [5].

During the 20<sup>th</sup> century various authors suggested expressions for the description of real gas effects. Numerous Equations of State (EoS) have been proposed in the literature on empirical, semiempirical or theoretical basis. The van der Waals EoS was the first equation to approximate the real gas behavior [6]. This correlation was the first model to take into account the volume of molecules and their interactions, as well as describing qualitatively the basic properties of a real gas. Later on, Redlich-Kwong EoS [7] improved the accuracy of the van der Waals equation including a temperature's dependence in the attractive term. Soave *et al.* [8], [9] and Peng and Robinson *et al.*[10] proposed additional modifications of the Redlich-Kwong equation to predict more accurately the vapor pressure, liquid density and equilibrium ratios. These equations are called cubic equations of state and they represent and predict pure components thermodynamic properties. These equations are widely used in several industrial applications. This kind of equations require specific data like critical pressure and temperature for each pure specie. Kouremenos *et al.*[13] developed a generalized analytic method based on different EoS for the calculation of real gas process. Three real isentropic exponents  $\gamma_{pv}$ ,  $\gamma_{Tv}$  and  $\gamma_{pT}$  replaced the classical isentropic exponent  $\gamma = Cp/Cv$  in the equation of the ideal gas isentropic process [11], [12] in order to calculate the normal and oblique stationary shock of real gases based on different EoS using these proposed correlations. An additional contribution of this study was the derivation of real gas shock wave equation, which is algebraically similar to the ideal gas shock wave equation [14] and [15].

Recently, the effects of real gas at high pressure have been investigated through CFD simulation. The results were applied to different industrial process, for instance: combustion [16], hydrogen realize at high pressure [17], etc.

In the present paper, real gas effects of R245fa are analyzed in the expansion processes commonly used in ORC. The NIST database was used as a reference to estimate the accuracy of the selected EoS gas models. An isothermal process, followed by an isochoric process are proposed to reproduce the thermodynamic process of the organic fluid expansion, by simpler equations. So, the thermodynamic parameters obtained directly from the EoS (pressure, temperature and density) and other thermodynamic functions (specific heats, speed of sound, internal energy, entropy and enthalpy) must be determined to achieve this goal. Thus, this paper has two main sections:

In the first section, different EoS are evaluated. Then, the complexity and accuracy of equations are compared and discussed. The criteria to analyze the results is based on the minimum relative deviation between predicted pressure by EoS proposed work and NIST database [18] (National Institute of Standards and Technology). NIST database have been obtained by Helmholtz energy equations of state previously fitted by Lemmon *et al.* [19]. The proposed EoS are derived to calculate specific heats and speed of sound. Finally, differential variations of internal energy, entropy and enthalpy are estimated using ideal and real models, in order to calculate the variations of these parameters on different processes. All these calculated parameters have been compared with NIST database to estimate the models accuracies.

In the second section, the proposed EoS are used to calculate the specific output energy in typical expansion process of ORC (2.5 MPa-0.1 MPa and 1.6MPa-0.1MPa).

## 2. Study of real-gas state equation of R245fa

The simplest EoS is the ideal gas equation. An ideal gas is defined as one in which all collisions between molecules are perfectly elastic and in which there are no intermolecular attractive forces.

In the typical ORC expansion process with R245fa, the inlet pressure is near to the critical pressure (the intermolecular effects are increased in this critical region) and the temperature level is high enough to underestimate the molecular volume. Because of these deviations, a supercritical ORC or a high evaporation temperature cycle should not be studied with the ideal gas laws. When pressures and temperatures decrease below the critical zone, the intermolecular effects are becoming increasingly negligible.

A comparison of the NIST R245fa database with the obtained results by R245fa ideal gas has been performed in this range. Figure 1 shows the pressure relative deviation between the NIST database and the ideal gas model. The ORC temperature and pressure ranges in the present work are set to 450-300 K and 3.64-0.1 MPa respectively. The ideal gas equation implies an deviation in typical ORC expansion ranges from 5% to 100% (450 K-300 K). Therefore, it is not possible to use an ideal gas approximation for these studies, thus a real gas model should be used. When the ideal gas model is used, it is possible to observe that as pressure is reduced, the relative pressure deviation decreases. Finally, the deviation of the ideal gas model is negligible close to the ambient pressure (0.1 MPa).

In the literature, there are real gas models for refrigerants of varying complexity [20] and [21]. They can be used to model the thermophysical properties in conditions where the ideal assumptions can not be considered. Among these models, cubic equations are the most popular because of their relative simplicity and their low computational cost [22]. The Redlich-Kwong-Soave and the Peng-Robinson EoS will be used to evaluate their accuracy in calculating the thermophysical variables of R245fa as well as their application in calculating power output in an ORC.

The Redlich-Kwong EoS (RK) was introduced in 1949. It is a modification of van der Waals equation and has several restrictions close to the saturated vapor curve. Redlich-Kwong-Soave equation (RKS) improves the RK equation in order to fit the vapor pressure for hydrocarbons. This new correlation includes a temperature dependent parameter to better reproduce the saturated vapor line but with significant deviation in the vicinity to the critical point. RKS equation is defined with the following equations:

$$P = \frac{RT}{v-b} - \frac{a}{v} \frac{\alpha(T)}{v+b} \quad (1)$$

Where:

$$a = \frac{0.42747R^2T_c^2}{P_c} \quad b = \frac{0.008664RT_c}{P_c}$$

$$\alpha(T) = \left(1 + \alpha_{RKS} \left(1 - \sqrt{\frac{T}{T_c}}\right)\right)^2$$

$$\alpha_{RKS} = 0.48 + 1.574\omega - 0.176\omega^2$$

Peng-Robinson (PR) equation is one of the most utilized equations in pure substance studies. It represents an improvement of the van der Waals, RK and RKS EoS, overall on the liquid phase density prediction close to the critical point. It is defined with the following equations:

$$P = \frac{RT}{v-b} - \frac{\alpha(T) \cdot a}{v^2 + 2bv - b^2} \quad (2)$$

Where:

$$a = \frac{0.452724R^2T_c^2}{P_c} \quad b = \frac{0.07780RT_c}{P_c}$$

$$\alpha(T) = \left(1 + \alpha_{PR} \left(1 - \sqrt{\frac{T}{T_c}}\right)\right)^2$$

$$\alpha_{PR} = 0.37464 + 1.54226\omega - 0.26992\omega^2$$

All the parameters needed to define these equations of state are typical parameters of each fluid. These parameters obtained by NIST database [23] of the fluid R245fa are listed in Table 1.

Equations (1) and (2) define the RKS and PR EoS, respectively, and they can be calculated for the R245fa using the parameters of Table 1. Thus, the pressure in this fluid can be easily obtained from these equations by determining the temperature and specific volume. Finally, the relative deviation of pressure can be obtained by comparing these

pressures with the NIST data base. Figure 2 shows relative deviations of pressure with respect to NIST database, when RKS and PR EoS are used.

The RKS equation gives a good approximation at temperatures and pressures lower than the critical condition . Its relative pressure deviation at common working point in ORC is around 1.8 % (close the saturated vapor line) and 0.25 % (close to 0.1 MPa). Because of this, RKS can be considered an important improvement respect to the ideal gas law.

On the other hand, PR equation presents a pressure relative deviation lower than 1 % along the saturated vapor line, (even in the critical point). This is a reason for using the PR equation in a supercritical ORC. On subcritical conditions, RKS and PR have similar deviations as shown in Figure 2.

### 3. Thermodynamic variables analysis

The compressible flow behavior is essential to model ORC expansion processes, due to their high expansion ratios. Thus, it is essential to estimate the thermodynamic parameters of R245fa, due to their importance in compressible flow behavior. The thermodynamic properties of a compressible flow (specific heat, speed of sound, specific internal energy, specific enthalpy and specific entropy) must be estimated as precisely as possible in order to obtain an adequate real gas model to calculate supersonic flow processes. These real gas properties are defined in literature [24] as:

$$C_v = C_{vi} + T \int_{\infty}^v \frac{\partial^2 P}{\partial T^2} dv \quad (3)$$

$$C_p = C_v - T \frac{\frac{\partial P}{\partial T}}{\frac{\partial P}{\partial v}} \quad (4)$$

$$c = \sqrt{\frac{\partial p}{\partial \rho}} = \sqrt{-v^2 \frac{\partial P}{\partial v}} \quad (5)$$

$$\partial e = C_v \partial T + \left( T \frac{\partial P}{\partial T} - P \right) \partial v \quad (6)$$

$$\partial h = C_p \partial T + \left( T \frac{\partial P}{\partial T} - P \right) \partial v \quad (7)$$

$$\partial s = \frac{\partial s}{\partial T} \partial T + \frac{\partial s}{\partial v} \partial v = C_v \frac{\partial T}{T} + \frac{\partial P}{\partial T} \partial v \quad (8)$$

Equations (3), (4) and (5) allow a direct calculation of the specific heat capacities ( $C_p$  ,  $C_v$ ) and the speed of sound ( $c$ ). The differential internal energy ( $\partial e$ ), differential enthalpy ( $\partial h$ ) and differential entropy ( $\partial s$ ) are obtained through differential parameter calculation in equations (6), (7) and (8) . Consequently, it is possible to calculate these parameters ( $e$ ,  $h$  and  $s$ ) at any point, if they are known at a reference point. On the other hand, all these equations can be defined as expressions dependent on temperature variations and specific volume variations. However, the

direct solution of these equations can often involve complex equations that are difficult to calculate. To simplify the resolution of these equations, all thermodynamic state functions can be calculated as the sum of two processes, from a reference point, where all the properties are known, to the point that must be calculated. Figure 3 shows the path proposed in the literature [24] to calculate the thermodynamic parameters. The first process is an isochoric ideal process from a reference point -1- to the temperature of the calculated point -1'- and the second process is an isothermal process from this point to the calculated point -2-.

As seen in previous section, R245fa behaves as an ideal gas at very low pressure conditions. This zone is the white area on the bottom right in Figure 3. In this zone, it is possible to calculate the thermodynamic parameters from a reference point as an isochoric ideal process.

However, this fluid has a non-ideal behavior in the gray area at the top left in the figure. Thus, the second process should be calculated as an isothermal process of a real gas. The reference point  $P=1$  Pa and  $T=200$  K through the isochoric line  $v=12,405\text{m}^3/\text{kg}$  is chosen in this study to use as a basis for the calculation of the thermodynamic parameters.

### 3.1. Specific heat capacities and speed of sound in real gases

The specific heat capacity at constant pressure on the reference isochoric process can be estimated with a correlation, which can be calculated using the NIST database. In this study, we used a 3rd degree polynomial which has been correlated with temperatures in order to estimate the specific heat capacity at constant pressure in terms of quasi-ideal gas state ( $C_{pi}$ ). This correlation has been fitted using data from NIST data base through the isochoric line  $v=12,405\text{m}^3/\text{kg}$  and from 200 K to 450 K. Equation (9) is the result of such correlation, where the temperature is expressed in Kelvin and the specific heat capacity at constant pressure in J/(kgK).

$$C_{pi} = 354.65 + 117.25 \times 100^{-1}T + 28.27 \times 100^{-2}T^2 + 3.67 \times 100^{-3}T^3 \quad (9)$$

This correlation has a maximum relative deviation near 0.80 % over the NIST database, in the isochoric line  $v=12,405\text{m}^3/\text{kg}$ .

Considering  $R = C_{pi} - C_{vi}$  and the equation (3), it is possible to obtain the equation (10).

$$C_v = C_{pi} - R + T \int_{\infty}^v \frac{\partial^2 p}{\partial T^2} dv \quad (10)$$

Thus,  $C_p$  can be obtained calculating the value of  $C_v$  from the equation (3) and substituting this value in equation (4). Moreover, from equation (5) and taking into account the relation (11), it is possible to obtain speed of sound as shown in equation (12).

$$\left. \frac{\partial p}{\partial v} \right|_{s=cte} = \frac{C_p}{C_v} \frac{\partial p}{\partial v} \quad (11)$$



$$c = \sqrt{-v^2 \frac{C_p}{C_v} \frac{\partial p}{\partial v}} \quad (12)$$

The thermodynamic relations (4), (10) and (12) to calculate specific heat capacities and speed of sound are described in derivative and integrals terms of the EoS. Table 2 contains analytical expression of derivatives and integrals for the different EoS considered in this work.

Then, it is possible to calculate specific heat capacities and speed of sound using the equations (4), (10), (12) and the expressions of Table 2. Thus, three different models (Ideal gas, RKS and PR) can be used to obtain these parameters depending on the EoS used. Figure 4 shows relative deviations between these models and the NIST database values on the studied zone.

The results calculated by the models of RKS, PR and ideal gas show a relative deviation which increases when approaching to the critical point. The ideal gas model generates a maximum relative deviation of 100 %, 70 % and 70 % for  $C_v$ ,  $C_p$  and speed of sound respectively. Hence, the ideal hypothesis should not be applied to the calculations on typical expansions ranges of ORC, especially near the critical point. The models of PR and RKS have a similar accuracy near to the saturated mixture zone with maximum deviation of 10 %, 20 % and 5 % for  $C_v$ ,  $C_p$  and  $c$  respectively. Close to the critical pressure and 450 K, RKS equation is more appropriate as result of its low deviations especially in the calculation of  $C_p$  (5%).

### 3.2. Specific internal energy, specific enthalpy and specific entropy

As it was previously introduced, equations (6),(7) and (8) allow calculating differential parameters of variables such as differential internal energy ( $\partial e$ ), differential enthalpy ( $\partial h$ ) and differential entropy ( $\partial s$ ). Consequently, integrating equations (6), (7) and (8) from the reference point **-1-** to the calculated point **-2-**, defined previously in Figure 3, it is possible to obtain equations (13), (14) and (15). This integration has been done following the two proposed processes, first an isochoric process from **-1-** to **-1'**- and after an isothermal process from **-1'**- to **-2-**.

$$e_2 - e_1 = \int_{T_1}^{T_2} C_{vi} \partial T \Big|_{v=v_1} + \int_{v_1}^{v_2} \left( T \frac{\partial P}{\partial T} - P \right) \partial v \Big|_{T=T_2} \quad (13)$$

$$h_2 - h_1 = \int_{T_1}^{T_2} C_{pi} \partial T \Big|_{P=P_1} + \int_{v_1}^{v_2} \left( T \frac{\partial P}{\partial T} - P \right) \partial v \Big|_{T=T_2} \quad (14)$$

$$s_2 - s_1 = \int_{T_1}^{T_2} C_{vi} \frac{\partial T}{T} \Big|_{v=v_1} + \int_{v_1}^{v_2} \left( \frac{\partial P}{\partial T} \right)_v \partial v \Big|_{T=T_2} \quad (15)$$

In conclusion, knowing the internal energy, enthalpy and entropy at a reference point **-1-**, it is possible to calculate these parameters at any point **-2-** using equations (13), (14) and (15). Table 3 contains the analytical expressions of derivatives and integrals used for different EoS equations in this work.

Figure 5 shows the relative deviation of the differential internal energy and differential enthalpy obtained using equations (13) and (14) and the expressions of Table 3. If it is compared with the NIST database, the ideal gas equation

generates also the maximum deviations, between 10-60 % in each variable. The relative deviation distribution of RKS and PR equation is similar to that of the previous section, they generate lower deviations as compared to that of the EoS of ideal gas. EoS of RKS and PR have relative deviations lower than 2.5%. The PR is a good approximation along the saturated vapor line, but RKS being the most accuracy equation close the critical pressure and high temperatures.

#### 4. Calculation of the specific output energy in ORC

An organic Rankine cycle usually presents a high pressure ratio between evaporator and condenser conditions, so the fluids used in these expansion processes could reach supersonic conditions [5]. Many times, the expansion machine selected is an axial flow impulse turbine (Laval Turbine). The design of these turbines considers high expansion ratios because essentially all the expansion process occurs in the nozzles. An expansion in an impulse turbine is selected for the purpose of evaluating the accuracy of the studied EoS in order to calculate the power output in turbines which are often installed in ORC.

Figure 6 shows two expansion processes considered in the present study in a  $T - s$  diagram, both the isentropic and non-isentropic processes in the turbine. It is considered: state **1** at inlet turbine conditions; **2s** at outlet turbine conditions in an isentropic expansion process and **2** at outlet turbine conditions in a non-isentropic expansion process. A 70 % of isentropic efficiency is considered in the non-isentropic expansion process. Point **B** is located where the influence of real gas behavior is high but not too close to the saturated mixture region. Point **A** is selected very close to the saturated vapor line and the critical point where the state equations are less accurate as shown in previous studies. From each point, a set of expansion processes is calculated from these high pressure conditions to different outlet pressure conditions (close to 0.1 MPa) in order to evaluate expansion processes frequently used in ORC with R245fa as working fluid [25], [26].

Figure 7 a) shows the specific energy of the fluid obtained from the calculation of these expansion processes with **B** as initial operation point considering the different EoS studied in this paper. As shown in figure 7 a), the ideal gas equation is highly inaccurate in the calculation of the energy obtained by the process of expansion (enormously higher than the NIST database). Figure 7 b) and c) show the relative and the absolute deviation respectively of the PR and RKS compared to the results obtained by NIST database. As it can be observed in figure 7 b) and c) , the accuracy of RKS and PR is acceptable at expansion processes with pressure ratios higher than 5 (from 6 % to 10 % and an absolute deviations about 3.5-3 kJ/kg). RKS is more accurate than PR at expansion processes with pressure ratio processes lower than 5 (12% vs 13 % relative deviation respectively). These accuracies are consistent with the results presented in Figure 5.

Figure 8 a) shows the specific output energy of different expansion processes from the initial point **A**. As shown in Figure 8 b) and c) , the accuracies of PR and RKS are similar throughout the different expansion processes. RKS is slightly more accurate than PR with an absolute value of 3.7 vs 3 kJ/kg respectively. The relative deviation is from 7% to 14 % in processes with expansion ratios higher than 5.

## 5. Effect of the EoS selected in the preliminary design of the expander in an ORC

ORC with R245fa as working fluid is one of the most popular solutions to produce electricity from low temperature waste heat sources. The temperatures of the hot and cold sources are usually ambient temperatures and low temperature sources between 450 K and 300 K, respectively. The evaporator and condenser pressures associated to these temperature levels are about 1.0 MPa and 2.5 MPa. When these parameters have been fixed, the study of the specific output energy produced is the next step that the ORC designers must consider in the implantation of the cycle. The selection of an accurate EoS is of crucial importance in the evaluation of the thermodynamic variables at the inlet and outlet conditions of the expander. The inaccuracies in the calculation of specific output energy can produce significant errors predicting the working fluid mass flow and the sizing of the heat exchangers, the pump and the expander.

A case of the implementation of a recovery system using low temperature heat sources at 420 K has been done, in order to illustrate the effect of the EoS selection in the calculation of the specific output energy in a typical ORC. For this study, the following hypothesis are imposed:

- The proposed cycle keeps a minimum temperature difference in the heat exchange processes fixed to 10 K [25], [26].
- The working fluid in the condenser is cooled by the atmospheric conditions (300 K).
- A Superheating of 15 K is assumed.
- An isentropic efficiency of 70% is imposed for the expansion machine.

Taking into account these hypothesis, the pressure level in the evaporator and condenser are 1.6 MPa and 0.16 MPa respectively, in other words, the pressure ratio in the expansion process is 10. As shown in Figure 8 the specific output energy is above 42 kJ/kg for NIST and PR, and 38 kJ/kg for RKS EoS. However, the ideal gas equation predicts a specific output energy enormously high (above 100 kJ/kg). For this, the RKS and PR can be considered in the preliminary calculation of the implementation of an ORC as recovering waste heat sources system, because the ideal gas equation can introduce significant deviations in the preliminary design.

Finally, the working fluid usually reaches supersonic conditions in the expander due to the high pressure ratios. For this, a good accuracy in the calculation of the thermodynamic variables and speed of sound can be necessary, in order to achieve greater detail of the compressible behaviors of the fluid in the expansion process.

## 6. Conclusions

A methodology to calculate the expansion process with enough accuracy in an ORC is proposed in this paper. An isothermal process, followed by an isochoric process are proposed to reproduce this thermodynamic process of the organic fluid expansion, by simple equations.

The real gas effects were considered in a typical expansion processes of an ORC. This study has ruled out the possibility of using EoS of ideal gas in the working conditions of a common ORC using R245fa, due to its low accuracy with the thermodynamics variables. To estimate the pressure, ideal gas EoS presents relative deviations that reach 80 %. On other hand, the RKS and PR EoS have better approximations without a high computational cost. These models present relative deviations in pressure lower than 2 % as Table 4 shows. Table 4 is a summary that shows their maximum relative deviations. The ideal gas model presents the highest relative deviations that exceed 100 % to predict  $C_v$  and 70 % to predict  $C_p$  and speed of sound. The RKS model presents relative deviations lower than 15 %, 20 % and 5% to predict  $C_v$ ,  $C_p$  and speed of sound respectively. The model of PR presents a similar accuracy except close to the critical point at high temperature where a high relative deviation is obtained to predict  $C_p$ .

A method to estimate differential parameters has been exposed and it has been used to calculate internal energy and enthalpy. The ideal gas model presents the highest relative deviations that reach up to 50 % to predict these parameters. However, the RKS and PR models present relative deviations lower than 2.5 %.

Finally, several expansion processes from two different initial conditions are studied using the studied EoS in order to evaluate their accuracy with the specific output energy in typical expansion processes of an ORC. These initial conditions are point **A** (1.6 MPa and low superheating conditions) and point **B** (2.5 MPa and high superheating conditions). In these calculations high inaccuracies are again obtained using ideal gas hypothesis. However, RKS and PR have lower deviations. These deviations are from 6% to 10 % in processes with expansion ratios higher than 5 and high superheating conditions (point **B**) and from 7% to 14% in processes with expansion ratios higher than 5 and low superheating conditions (point **A**). The deviations in high superheating conditions are lower, because the real gas behavior is becoming less intensive.

## 7. Acknowledgements

This work was partially funded by the "Programa de Formación de Profesorado Universitario (F.P.U)", "Programa de Apoyo a la Investigación y Desarrollo de la Universidad Politécnica de Valencia 2010", "Proyectos I+D para grupos de investigación emergentes 2011" and "Programa de apoyo a la investigación y desarrollo de la U.P.V (PAID-06-09)". The authors thanks to R. Gatzweiler for his help to improve the English grammar.

## References

### References

- [1] A.Schuster, S.Karellas, E.Kakaras, H.Spliethoff, Energetic and economic investigation of Organic Rankine Cycle applications, *Applied Thermal Engineering (ATE)* 29 (2009) 1809–1817.
- [2] U.Drescher, D.Brüggemann, Fluid selection for the Organic Rankine Cycle (ORC), in biomass power and heat plants, *Applied Thermal Engineering (ATE)* 27 (2007) 223–228.
- [3] F.Heberle, D.Brüggemann, Exergy based fluid selection for a geothermal Organic Rankine Cycle for combined heat and power generation, *Applied Thermal Engineering (ATE)* 20 (2010) 1326–1332.
- [4] V.Maizza, A.Maizza, Working Fluid in non-steady flow for waste energy recovery systems, *Applied Thermal Engineering (ATE)* 16 (1996) 579–590.
- [5] H.C.Man, J.Duana, T.M Yue, Design and characteristic analysis of supersonic nozzles for high gas pressure laser cutting, in: *Journal of Materials Processing Technology (JMPT)* 63 (1997) 217–222.
- [6] J.Murdock, W.James, *Fundamental fluid mechanics for the practicing engineer*, CRC Press, New York.1993.
- [7] O.Redlich, J.N.Kwong, On the Thermodynamics of Solutions. An Equation of State. Fugacities of Gaseous Solutions, *Chem. Rev* 44 (1949) 233–244.
- [8] G.Soave, Equilibrium constants from a modified Redlich-Kwong equation of state, in: *Chemical Engineering Science* 27 (1972) 1197–1203.
- [9] G.Soave, Rigorous and simplified procedures for determining the pure-component parameters in the Redlich-Kwong-Soave equation of state, *Chemical Engineering Science* 35 (1980) 1725–1730.
- [10] D.Y.Peng, D.B.Robinson Donald, A New Two-Constant Equation of State, *Ind. Eng. Chem. Fundamen.* 15 (1976) 59–64.
- [11] D.A.Kouremenos, X.K.Kakatsios, Ideal gas relations for the description of the real gas isentropic changes, *Forschung im Ingenieurwesen* 51 (1985) 169–174.
- [12] D.A.Kouremenos, X.K.Kakatsios, On the three exponents of the isentropic change of the refrigerant R22, *International Journal of Heat and Fluid Flow* 7 (1986) 199–207.
- [13] D.A.Kouremenos, K.A.Antonopoulos, Sound velocity and isentropic exponents for gases with different acentric factors by using the Redlich-Kwong-Soave equation of state, *Acta Mechanica* 66 (1987) 177–189.
- [14] D.A.Kouremenos, K.A.Antonopoulos, The normal shock waves of real gases and the generalized isentropic exponents, *Forschung im Ingenieurwesen* 52 (1986) 23–31.
- [15] D.A.Kouremenos, K.A.Antonopoulos, Generalized and exact solutions for oblique shock waves of real gases with application to real air, *International Journal of Heat and Fluid Flow* 10 (1989) 328–333.
- [16] M.Poschner, M.Pfützner, CFD-Simulation of supercritical LOX/GH2 combustion considering consistent real gas thermodynamics, *Proceedings of the European Combustion Meeting* (2009).
- [17] K.Mohamed, M.Paraschivoiu, Real gas simulation of hydrogen release from a high-pressure chamber, *International Journal of Hydrogen Energy* 8 (2009) 903–912.
- [18] On the Web: [www.webbook.nist.gov/chemistry/](http://www.webbook.nist.gov/chemistry/) March (2003).
- [19] E.W.Lemmon, R.Span, Short Fundamental Equations of State of 20 Industrial Fluids, *J. Chem. Eng Data* 51 (2006) 785–850.
- [20] B.Saleh, M.Wendland, Screening of pure fluids as alternative refrigerants, *International Journal of Refrigeration* 29 (2006) 260–269.
- [21] P.Colonna, S.Rebay, J.Harinck, A.Guardone, Real gas effects in ORC turbine flow simulations: influence of thermodynamic models on flow fields and performance parameters, *Proceedings of the ECCOMAS CFD 2006 Conference*, Egmond aan Zee, (The Netherlands), 2006.
- [22] N.A.Darwish, R.A.Al-Mehaideb, A.M.Braek, R.Hughes, Computer simulation of BTEX emission in natural gas dehydration using PR and RKS equation of state with different predictive mixing rules, *Environmental and Modelling and Software* 19 (2004) 957–65.

- [23] E.W. Lemmon, M.O. McLinden and D.G. Friend, Thermophysical Properties of Fluid Systems, NIST Chemistry WebBook, NIST Standard Reference Database Number 69, Eds. (2004) 957–965.
- [24] E.J. Richard and C.T. Lira, Introductory Chemical Engineering Thermodynamics, Pentice Hall, Upper Saddle River, NJ, 2001.
- [25] V. Dolz, R. Novella, A. García, J. Sánchez, HD Diesel engine equipped with a bottoming Rankine cycle as waste heat recovery system. Part 1: Study and analysis of the waste heat energy, Applied Thermal Engineering (ATE) (2011); doi:10.1016/j.applthermaleng.2011.10.025.
- [26] J.R. Serrano, V. Dolz, R. Novella, A. García, HD Diesel engine equipped with a bottoming Rankine cycle as waste heat recovery system. Part 2: Evaluation of alternative solutions, Applied Thermal Engineering (ATE) (2011); doi:10.1016/j.applthermaleng.2011.10.024.

## Nomenclature Acronyms

<i>CFD</i>	Computation Fluid Dynamic
<i>EoS</i>	Equation of State
<i>NIST</i>	National Institute of Standards and Technology
<i>ORC</i>	Organic Rankine Cycle
<i>RK</i>	Redlich-Kwong equation of state
<i>RKS</i>	Redlich-Kwong-Soave equation of state
<i>PR</i>	Peng-Robinson equation of state

## NOTATION

### Latin

<i>a, b, A, B, C, D</i>	constants
<i>c</i>	Speed of sound (m/s)
<i>C<sub>p</sub></i>	Specific heat capacity at constant pressure (J/kg/K)
<i>C<sub>v</sub></i>	Specific heat capacity at volume pressure (J/kg/K)
<i>E</i>	Total internal energy (J/kg).
<i>e</i>	Internal energy (J/kg).
<i>h</i>	Specific enthalpy (J/Kg)
<i>P</i>	Pressure (Pa)
<i>R</i>	Gas constant (J/kg/K)
<i>s</i>	Specific entropy (J/kg/K)
<i>T</i>	Temperature (K)
<i>v</i>	Specific volume ( $m^3/kg$ )

### Greek letters

$\alpha$	Attractive term
$\gamma$	Ideal specific heat ratio
$\rho$	Density ( $kg/m^3$ )
$\omega$	Acentric factor

### Subscripts

<i>c</i>	Critical thermodynamic variable
<i>i</i>	Quasi-ideal gas

*PR* Peng-Robinson

*RKS* Redlich-Kwong-Soave



- List of Tables

- Table 1. Properties of R245fa.
- Table 2. Analytical expressions of integrals and derivatives of EoS I.
- Table 3. Analytical expressions of integrals and derivatives of EoS II.
- Table 4. Maximum relative deviations of different thermodynamic parameters and calculation of specific energy in different expansion processes by ideal gas, RKS and PR equation.

- List of Figures

- Figure 1. Pressure relative deviation of R245fa by using ideal gas EoS.
- Figure 2. Pressure deviation of R245fa by using RKS and PR gas equation.
- Figure 3. Proposed pathway to calculate the thermodynamic parameters.
- Figure 4. Relative Deviation of  $C_v$ ,  $C_p$  and  $c$  by ideal gas, RKS and PR equation.
- Figure 5. Relative Deviation of internal energy and enthalpy by ideal gas, RKS and PR equation.
- Figure 6.  $T - s$  scheme for two different expansion processes (**A-B**) along an expander in an ORC.
- Figure 7. a) Specific output energy, b) relative and c) absolute deviation vs pressure ratio using different EoS with initial operative point fixed at **B**.
- Figure 8. c) Specific output energy, b) relative and b) absolute deviation vs pressure ratio using different EoS with initial operative point fixed at **A**.

Table 1: Properties of R245fa

Parameters	Value
Molecular Weight	134.0482 g/mol
Critical Temperature ( $T_c$ )	427.2 K
Critical Pressure ( $P_c$ )	3.64 MPa
Critical density ( $\rho_c$ )	517 $m^3/kg$
Acentric Factor	0.3724

Table 2: Analytical expressions of integrals and derivatives of EoS I

Variable	Ideal gas	RKS	PR
$\int_{\infty}^v \frac{\partial^2 P}{\partial T^2} dv$	0	$-\frac{a \alpha_{RKS} (1 + \alpha_{RKS}) \sqrt{\frac{T}{T_c}} \log \left[ \frac{v_2}{b + v_2} \right]}{2b}$	$-\frac{a(1 + \alpha_{PR}) \left( -1 + \left( -1 + \sqrt{\frac{T}{T_c}} \right) \alpha_{PR} \right) \log \left[ \frac{(-2 + \sqrt{2})b + \sqrt{2}v_2}{(2 + \sqrt{2})b + \sqrt{2}v_2} \right]}{2\sqrt{2}b}$
$\frac{\partial P}{\partial T}$	$\frac{R}{v}$	$\frac{R}{-b+v} + \frac{a \alpha_{RKS} \left( 1 + \alpha_{RKS} \left( 1 - \sqrt{\frac{T}{T_c}} \right) \right)}{\sqrt{\frac{T}{T_c}} T_c v (b+v)}$	$\frac{R}{-b+v} + \frac{a \alpha_{PR} \left( 1 + \alpha_{PR} \left( 1 - \sqrt{\frac{T}{T_c}} \right) \right)}{\sqrt{\frac{T}{T_c}} T_c (v^2 + 2bv - b^2)}$
$\frac{\partial^2 P}{\partial T^2}$	0	$-\frac{a \alpha_{RKS} (1 + \alpha_{RKS}) \sqrt{\frac{T}{T_c}}}{2T^2 v (b+v)}$	$-\frac{a \alpha_{PR} (1 + \alpha_{PR}) \sqrt{\frac{T}{T_c}}}{2T^2 (v^2 + 2bv - b^2)}$
$\frac{\partial P}{\partial v}$	$\frac{-RT}{v^2}$	$-\frac{RT}{(-b+v)^2} + \frac{a \left( 1 + \alpha_{RKS} \left( 1 - \sqrt{\frac{T}{T_c}} \right) \right)^2}{v (b+v)^2} + \frac{a \left( 1 + \alpha_{RKS} \left( 1 - \sqrt{\frac{T}{T_c}} \right) \right)}{v^2 (b+v)}$	$-\frac{RT}{(-b+v)^2} + \frac{a(2b+2v) \left( 1 + \alpha_{PR} \left( 1 - \sqrt{\frac{T}{T_c}} \right) \right)^2}{(v^2 + 2bv - b^2)^2}$

Table 3: Analytical expressions of integrals and derivatives of EoS II

EoS	Variable	Analytical expression
Ideal Gas	$\int_{\infty}^{\nu_2} \left( T \frac{\partial P}{\partial T} - P \right) \partial \nu$	0
	$\int_{\nu_1}^{\nu_2} \frac{\partial P}{\partial T} \partial \nu$	$R \log \left[ \frac{\nu_2}{\nu_1} \right]$
RKS	$\int_{\infty}^{\nu_2} \left( T \frac{\partial P}{\partial T} - P \right) \partial \nu$	$-\frac{a(\alpha_{RKS}+1)(\alpha_{RKS}(\sqrt{\frac{T}{T_c}}-1)-1) \log\left(\frac{\nu_2(b+\nu_1)}{\nu_1(b+\nu_2)}\right)}{b}$
	$\int_{\nu_1}^{\nu_2} \frac{\partial P}{\partial T} \partial \nu$	$\frac{a \alpha_{RKS} \left( \alpha_{RKS} T_c \sqrt{\frac{T}{T_c}} - \alpha_{RKS} T + T_c \sqrt{\frac{T}{T_c}} \right) \log\left(\frac{\nu_2(b+\nu_1)}{\nu_1(b+\nu_2)}\right) - b R T_c \log\left(\frac{b-\nu_1}{b-\nu_2}\right)}{b T T_c}$
PR	$\int_{\infty}^{\nu_2} \left( T \frac{\partial P}{\partial T} - P \right) \partial \nu$	$\frac{a \alpha_{PR} \sqrt{\frac{T}{T_c}} \left( \alpha_{PR} \left( -\sqrt{\frac{T}{T_c}} + \alpha_{PR} + 1 \right) \log\left( \frac{2\sqrt{2}b(\nu_1-\nu_2)}{b(b+(\sqrt{2}-1)\nu_2)-\nu_1(\sqrt{2}b+b+\nu_2)} + 1 \right) \right)}{2\sqrt{2}b}$
	$\int_{\nu_1}^{\nu_2} \frac{\partial P}{\partial T} \partial \nu$	$2a \left( \frac{1}{2(-b^2+2b\nu_1+\nu_1^2)} + \frac{1}{2b^2-4b\nu_2-2\nu_2^2} \right) \left( \alpha_{PR} \left( \sqrt{\frac{T}{T_c}} - 1 \right) - 1 \right)^2 + RT \left( \frac{1}{b-\nu_1} + \frac{1}{\nu_2-b} \right)$

Table 4: Maximum relative deviations of different thermodynamic parameters and calculation of specific output energy in different expansion process by ideal gas, RKS and PR equation

	P	$C_v$	$C_p$	c	e	h	Energy A	Energy A	Energy B	Energy B
							1.06 <sup>1</sup>	16 <sup>1</sup>	2.5 <sup>1</sup>	25 <sup>1</sup>
Equation of State										
Ideal gas	100%	100%	<70%	<70%	50%	50%	—	—	—	—
RKS	2%	15%	20%	5%	2.5%	2.5%	18%	7%	12%	6%
PR	2%	10%	20%	5%	2.5%	2.5%	22%	9%	13%	6%

<sup>1</sup> Pressure Ratio

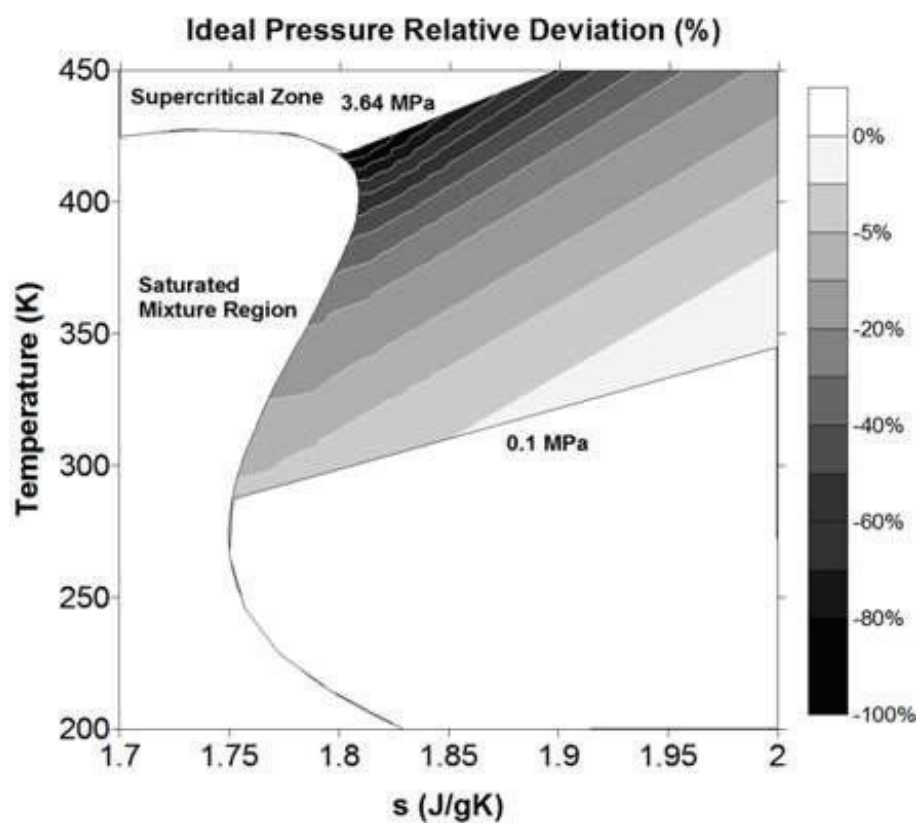


Figure 1: Pressure relative deviation of R245fa by using ideal gas equation

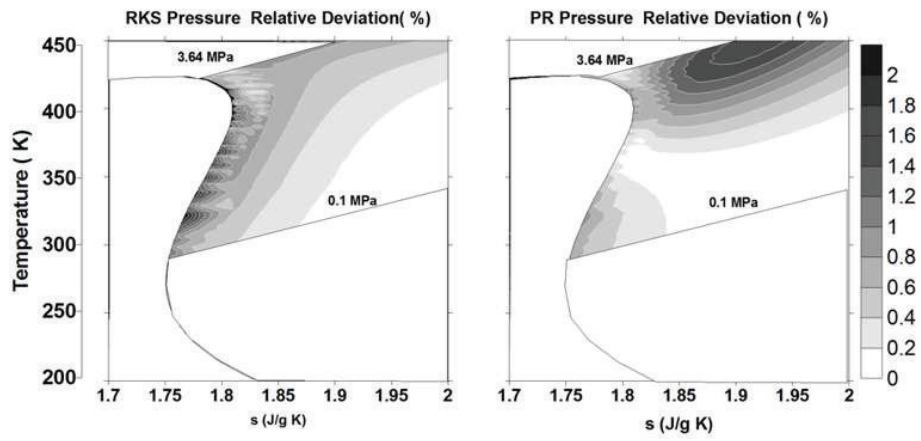


Figure 2: Pressure deviation of R245fa by using RKS and PR EoS

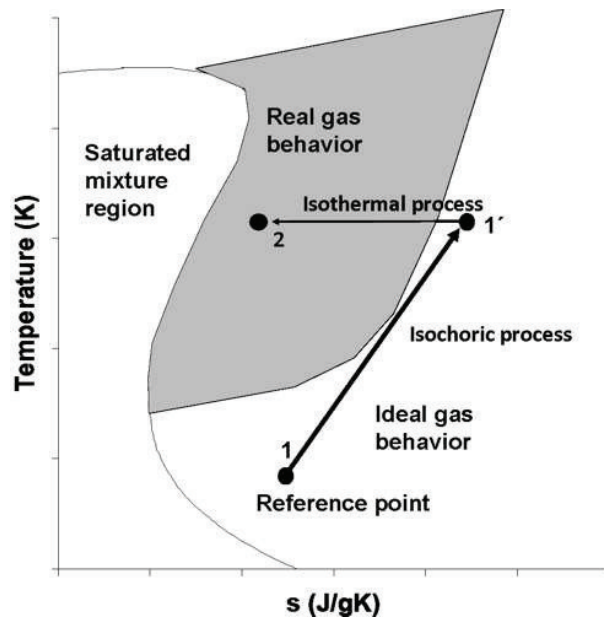


Figure 3: Proposed pathway to calculate the thermodynamic parameters



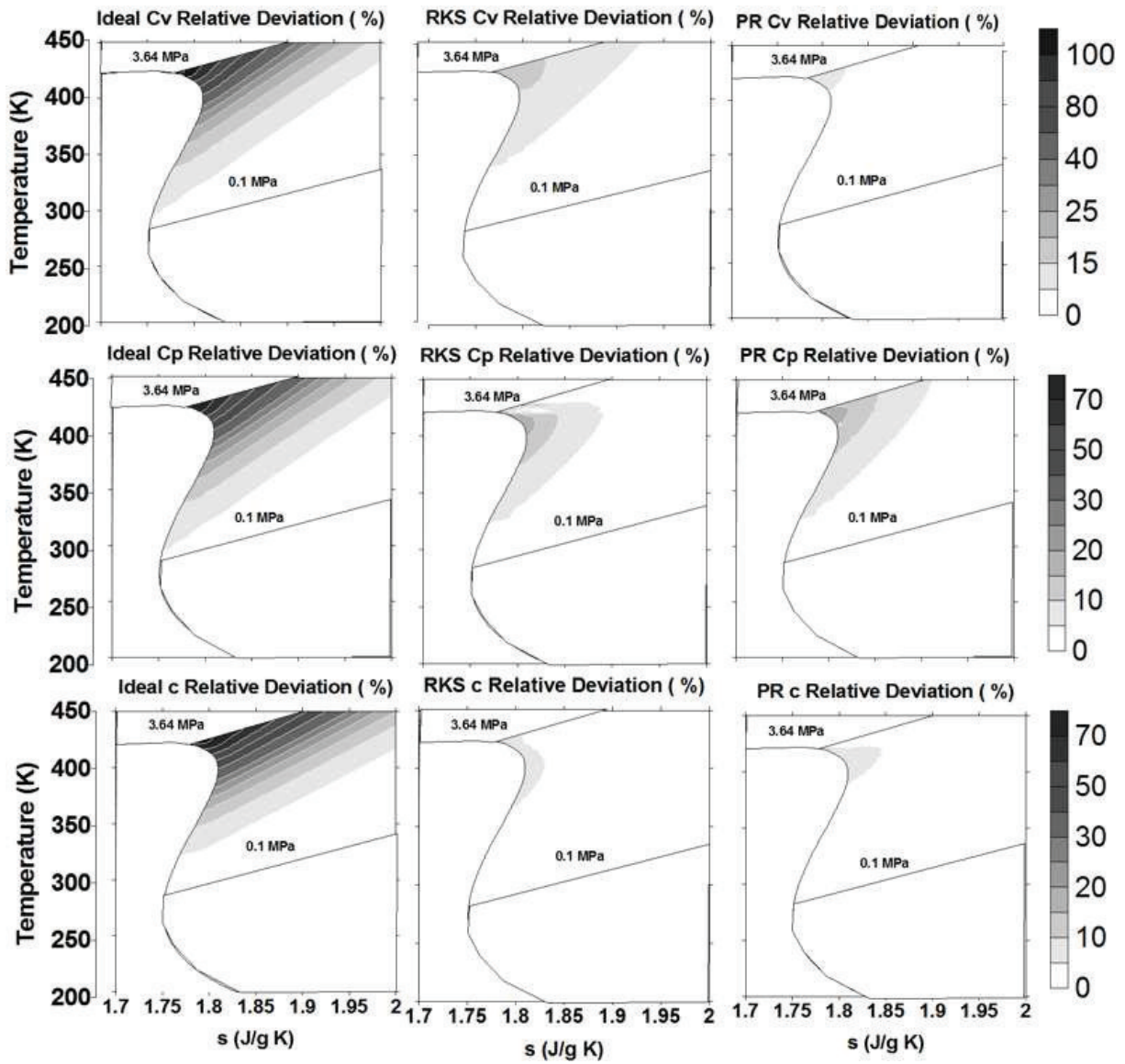


Figure 4: Deviation relative of  $C_v$ ,  $C_p$  and  $c$  by ideal gas, RKS and PR EoS

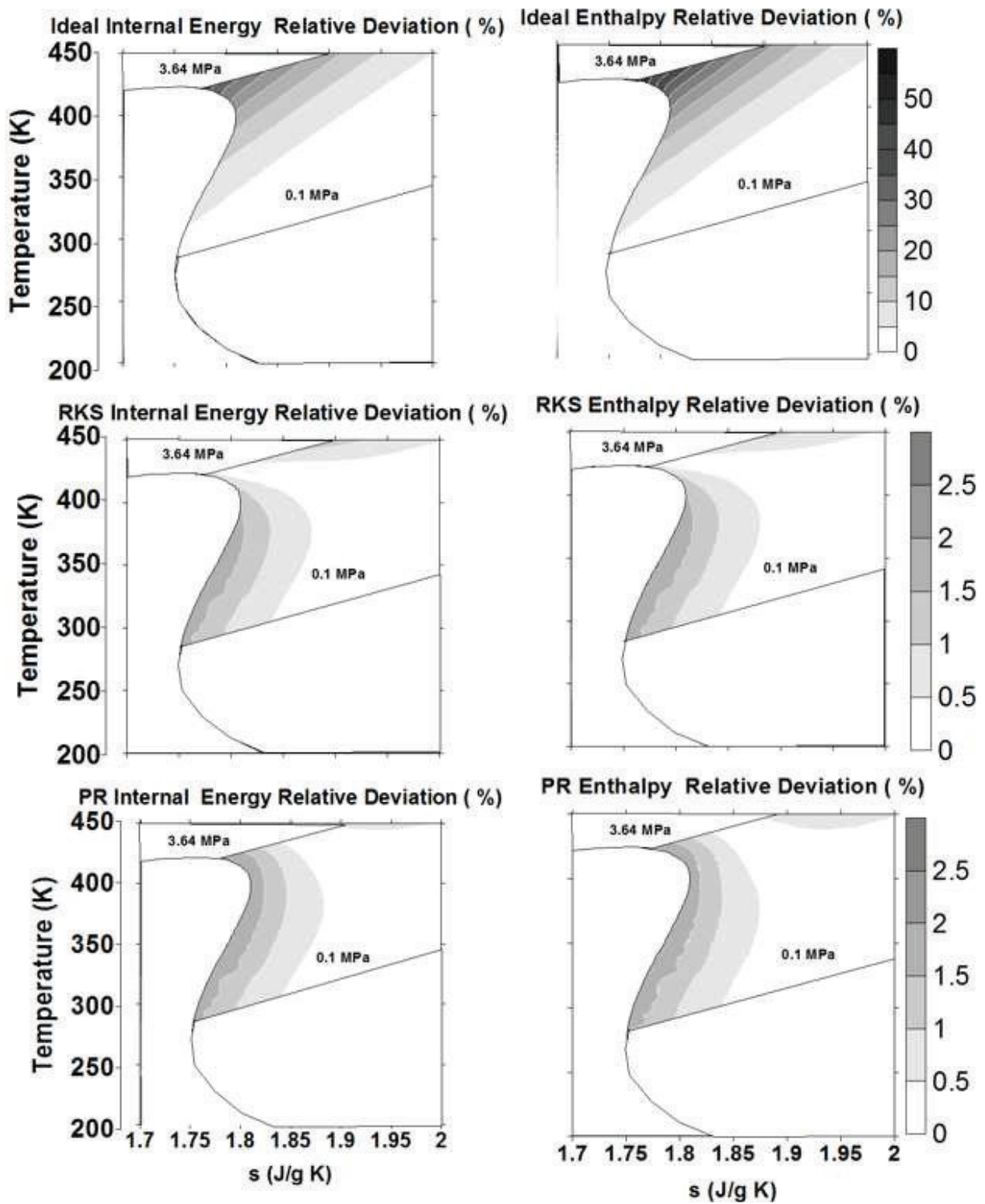


Figure 5: Deviation relative of internal energy and enthalpy by ideal gas, RKS and PR EoS

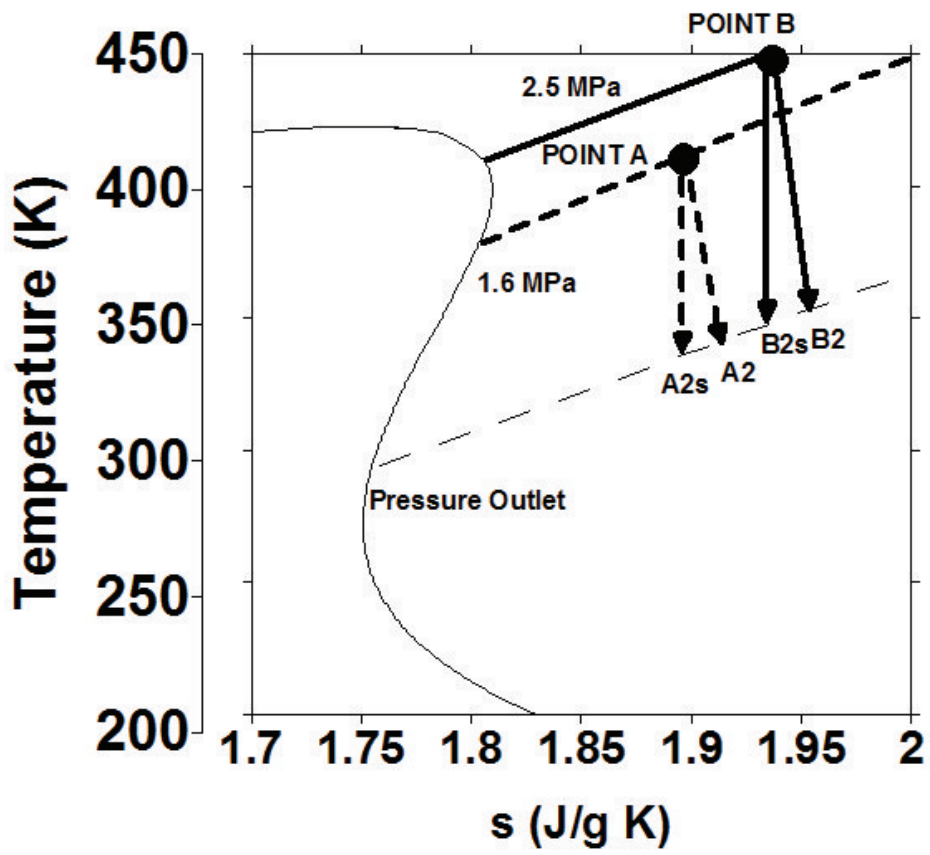


Figure 6:  $T - s$  scheme for two different expansion processes (A-B) in a common ORC

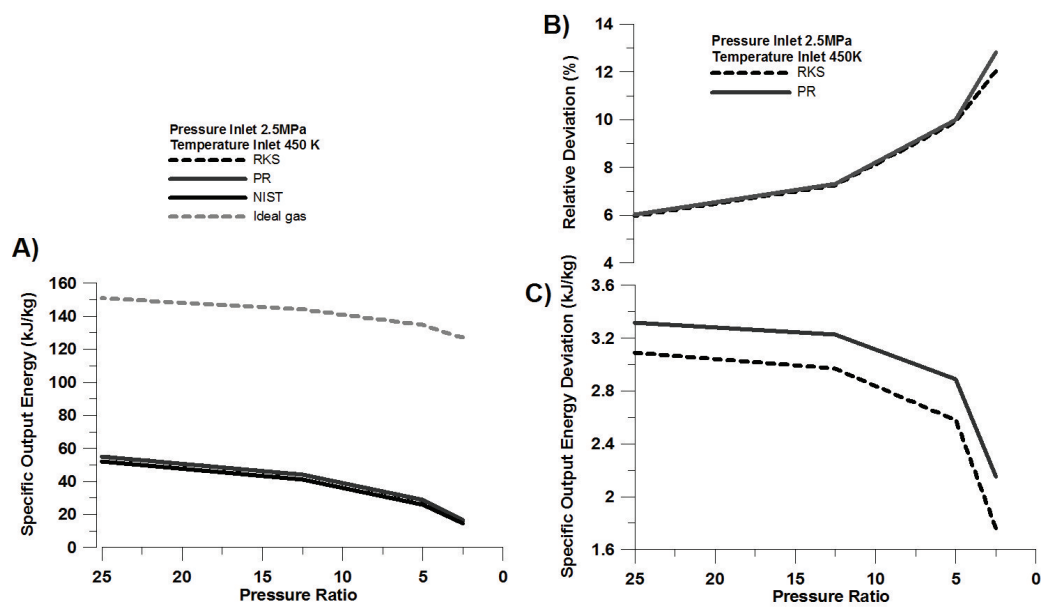


Figure 7: a) Specific output energy, b) relative and c) absolute deviation vs pressure ratio using different EoS with initial operative point fixed at **B**

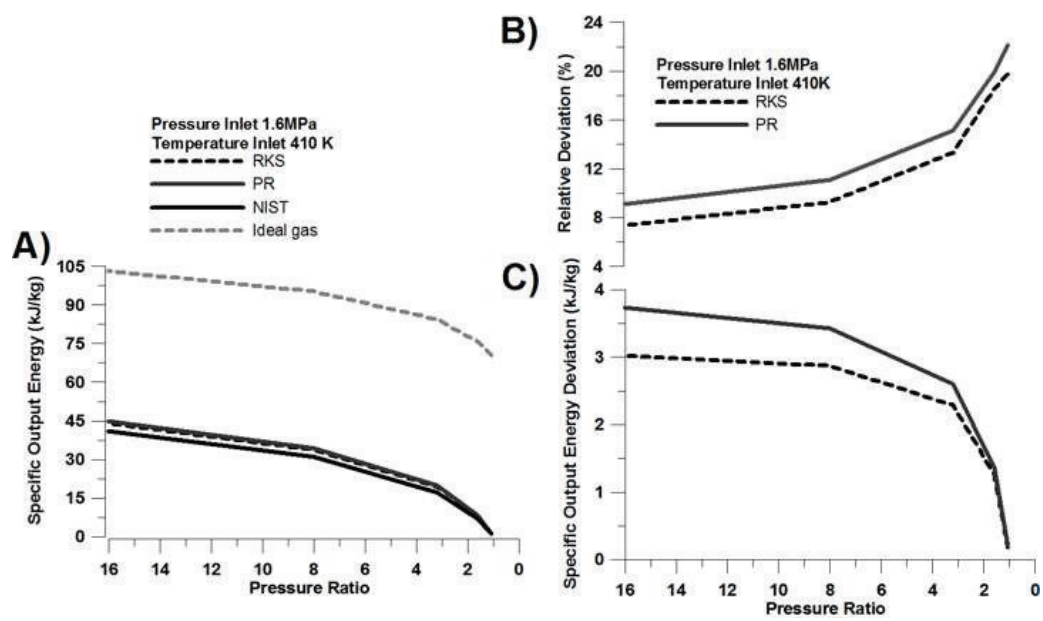


Figure 8: a) Specific output energy, b) relative and c) absolute deviation vs pressure ratio using different EoS with initial operative point fixed at A